

## LIGHT CURVES OF DWARF PLUTONIAN PLANETS AND OTHER LARGE KUIPER BELT OBJECTS: THEIR ROTATIONS, PHASE FUNCTIONS, AND ABSOLUTE MAGNITUDES

SCOTT S. SHEPPARD

Department of Terrestrial Magnetism, Carnegie Institution of Washington, 5241 Broad Branch Road NW, Washington, DC 20015, USA;  
sheppard@dtm.ciw.edu

Received 2006 September 25; accepted 2007 April 12

### ABSTRACT

I report new time-resolved light curves and determine the rotations and phase functions of several large Kuiper Belt objects, which includes the dwarf planet Eris (2003 UB<sub>313</sub>). Three of the new sample of 10 trans-Neptunian objects display obvious short-term periodic light curves. (120348) 2004 TY<sub>364</sub> shows a light curve which if double-peaked has a period of  $11.70 \pm 0.01$  hr and a peak-to-peak amplitude of  $0.22 \pm 0.02$  mag. (84922) 2003 VS<sub>2</sub> has a well-defined double-peaked light curve of  $7.41 \pm 0.02$  hr with a range of  $0.21 \pm 0.02$  mag. (126154) 2001 YH<sub>140</sub> shows variability of  $0.21 \pm 0.04$  mag with a possible  $13.25 \pm 0.2$  hr single-peaked period. The seven new Kuiper Belt objects in the sample which show no discernible variations within the uncertainties on short rotational timescales are (148780) 2001 UQ<sub>18</sub>, (55565) 2002 AW<sub>197</sub>, (119979) 2002 WC<sub>19</sub>, (120132) 2003 FY<sub>128</sub>, (136108) Eris 2003 UB<sub>313</sub>, (90482) Orcus 2004 DW, and (90568) 2004 GV<sub>9</sub>. Four of the 10 newly sampled Kuiper Belt objects were observed over a significant range of phase angles to determine their phase functions and absolute magnitudes. The three medium- to large-sized Kuiper Belt objects 2004 TY<sub>364</sub>, Orcus, and 2004 GV<sub>9</sub> show fairly steep linear phase curves ( $\sim 0.18$  to  $0.26$  mag deg<sup>-1</sup>) between phase angles of  $0.1^\circ$  and  $1.5^\circ$ . This is consistent with previous measurements obtained for moderately sized Kuiper Belt objects. The extremely large dwarf planet Eris (2003 UB<sub>313</sub>) shows a shallower phase curve ( $0.09 \pm 0.03$  mag deg<sup>-1</sup>) which is more similar to the other known dwarf planet Pluto. It appears that the surface properties of the largest dwarf planets in the Kuiper Belt may be different than the smaller Kuiper Belt objects. This may have to do with the larger objects' ability to hold more volatile ices, as well as sustain atmospheres. Finally, it is found that the absolute magnitudes obtained using the phase slopes found for individual objects are a few tenths of magnitudes different than that given by the Minor Planet Center.

*Key words:* Kuiper Belt — minor planets, asteroids — Oort Cloud — planets and satellites:  
individual ((148780) 2001 UQ<sub>18</sub>, (126154) 2001 YH<sub>140</sub>, (55565) 2002 AW<sub>197</sub>, (119979) 2002 WC<sub>19</sub>,  
(120132) 2003 FY<sub>128</sub>, (136199) Eris 2003 UB<sub>313</sub>, (84922) 2003 VS<sub>2</sub>, (90482) Orcus 2004 DW,  
(90568) 2004 GV<sub>9</sub>, and (120348) 2004 TY<sub>364</sub>) — solar system: general

*Online material:* machine-readable table

### 1. INTRODUCTION

To date only about 1% of the trans-Neptunian objects (TNOs) are known of the nearly 100,000 expected that are larger than about 50 km in radius just beyond Neptune's orbit (Trujillo et al. 2001). The majority of the largest Kuiper Belt objects (KBOs) now being called dwarf plutonian planets (radii > 400 km) have only recently been discovered in the last few years (Brown et al. 2005). The large self-gravity of the dwarf planets will allow them to be near hydrostatic equilibrium, have possible tenuous atmospheres, retain extremely volatile ices such as methane, and are likely to be differentiated. Thus, the surfaces as well as the interior physical characteristics of the largest TNOs may be significantly different than the smaller TNOs.

The largest TNOs have not been observed to have any remarkable differences from the smaller TNOs in optical and near-infrared broadband color measurements (Doressoundiram et al. 2005; Barucci et al. 2005). But near-infrared spectra have shown that only the three largest TNOs [Pluto, Eris (2003 UB<sub>313</sub>), and (136472) 2005 FY<sub>9</sub>] have obvious methane on their surfaces, while slightly smaller objects are either spectrally featureless or have strong water ice signatures (Brown et al. 2005; Licandro et al. 2006; Jewitt & Luu 2006; Trujillo et al. 2007). In addition to the near-infrared spectra differences, the albedos of the

larger objects appear to be predominately higher than those of the smaller objects (Cruikshank et al. 2005; Bertoldi et al. 2006; Brown et al. 2006). A final indication that the larger objects are indeed different is that the shapes of the largest KBOs seem to signify that they are more likely to be in hydrostatic equilibrium than the smaller KBOs (Sheppard & Jewitt 2002; Trilling & Bernstein 2006; Lacerda & Luu 2006).

The Kuiper Belt has been dynamically and collisionally altered throughout the age of the solar system. The largest KBOs should have rotations that have been little influenced since the sculpting of the primordial Kuiper Belt. This is not the case for the smaller KBOs, where recent collisions and fragmentation processes will have highly modified their spins throughout the age of the solar system (Davis & Farinella 1997). The large volatile-rich KBOs show a significantly different median period and a possible amplitude rotational differences when compared to the rocky large main-belt asteroids (MBAs), which is expected because of their differing compositions and collisional histories (Sheppard & Jewitt 2002; Lacerda & Luu 2006).

I have furthered the photometric monitoring of large KBOs (absolute magnitudes  $H < 5.5$  or radii greater than about 100 km assuming moderate albedos) in order to determine their short-term rotational and long-term phase-related light curves to better understand their rotations, shapes, and possible surface

TABLE 1  
OBSERVATIONS OF KUIPER BELT OBJECTS

Name	Image <sup>a</sup>	Air Mass	Exp. <sup>b</sup> (s)	UT Date <sup>c</sup>	Mag. ( $m_R$ ) <sup>d</sup>	Err. ( $m_R$ ) <sup>e</sup>
(148780) 2001 UQ <sub>18</sub> .....	uq1223n3025	1.17	320	2003 Dec 23.22561	22.20	0.04
	uq1223n3026	1.15	320	2003 Dec 23.23060	22.30	0.04
	uq1223n3038	1.02	320	2003 Dec 23.28384	22.38	0.04
	uq1223n3039	1.01	320	2003 Dec 23.28882	22.56	0.04
	uq1223n3051	1.01	350	2003 Dec 23.34333	22.40	0.04
	uq1223n3052	1.01	350	2003 Dec 23.35123	22.48	0.04
	uq1223n3070	1.15	350	2003 Dec 23.41007	22.37	0.04
	uq1223n3071	1.17	350	2003 Dec 23.41540	22.28	0.04
	uq1224n4024	1.21	350	2003 Dec 24.21433	22.30	0.03
	uq1224n4025	1.19	350	2003 Dec 24.21969	22.15	0.03

NOTES.—Table 1 is published in its entirety in the electronic edition of the *Astronomical Journal*. A portion is shown here for guidance regarding its form and content.

<sup>a</sup> Image number.

<sup>b</sup> Exposure time for the image.

<sup>c</sup> Decimal Universal Date at the start of the integration.

<sup>d</sup> Apparent red magnitude.

<sup>e</sup> Uncertainties on the individual photometric measurements.

characteristics. This is a continuation of previous works (Jewitt & Sheppard 2002; Sheppard & Jewitt 2002, 2003, 2004).

## 2. OBSERVATIONS

The data for this work were obtained at the Dupont 2.5 m telescope at Las Campanas in Chile and the University of Hawaii 2.2 m telescope atop Mauna Kea in Hawaii.

Observations at the Dupont 2.5 m telescope were performed on the nights of 2005 February 14, 15, and 16, March 9 and 10, October 25, 26, and 27, November 28, 29, and 30, and December 1 UT. The instrument used was the Tek5 with a 2048 × 2048 pixel CCD with 24 μm pixels giving a scale of 0.259'' pixel<sup>-1</sup> at the f/7.5 Cassegrain focus for a field of view of about 8.85' × 8.85'. Images were acquired through a Harris R-band filter while the telescope was autoguided on nearby bright stars at sidereal rates (Table 1). Seeing was generally good and ranged from 0.6'' to 1.5'' FWHM.

Observations at the University of Hawaii 2.2 m telescope were obtained on the nights of 2003 December 19, 21, 23, and 24, UT and used the Tektronix 2048 × 2048 pixel CCD. The pixels were 24 μm in size, giving a 0.219'' pixel<sup>-1</sup> scale at the f/10 Cassegrain focus for a field of view of about 7.5' × 7.5'. Images were obtained in the R-band filter based on the Johnson-Kron-Cousins system with the telescope autoguiding at sidereal rates using nearby bright stars. Seeing was very good over the several nights ranging from 0.6'' to 1.2'' FWHM.

For all observations the images were first bias subtracted and then flat-fielded using the median of a set of dithered images of the twilight sky. The photometry for the KBOs was done in two ways in order to optimize the signal-to-noise ratio. First, aperture correction photometry was performed by using a small aperture on the KBOs (0.65''–1.04'' in radius) and both the same small aperture and a large aperture (2.63''–3.63'' in radius) on several nearby unsaturated bright field stars. The magnitude

TABLE 2  
PROPERTIES OF OBSERVED KBOs

Name	$H^a$ (mag)	$m_R^b$ (mag)	No. Nights <sup>c</sup>	$\Delta m_R^d$ (mag)	Single <sup>e</sup> (hr)	Double <sup>f</sup> (hr)
(148780) 2001 UQ <sub>18</sub> .....	5.4	22.3	2	<0.3	...	...
(126154) 2001 YH <sub>140</sub> .....	5.4	20.85	4	0.21 ± 0.04	13.25 ± 0.2	...
(55565) 2002 AW <sub>197</sub> .....	3.3	19.88	2	<0.03	...	...
(119979) 2002 WC <sub>19</sub> .....	5.1	20.58	4	<0.05	...	...
(120132) 2003 FY <sub>128</sub> .....	5.0	20.28	2	<0.08	...	...
(136199) Eris 2003 UB <sub>313</sub> .....	-1.2	18.36	7	<0.01	...	...
(84922) 2003 VS <sub>2</sub> .....	4.2	19.45	4	0.21 ± 0.02	...	7.41 ± 0.02
(90482) Orcus 2004 DW.....	2.3	18.65	5	<0.03	...	...
(90568) 2004 GV <sub>9</sub> .....	4.0	19.68	4	<0.08	...	...
(120348) 2004 TY <sub>364</sub> .....	4.5	19.98	7	0.22 ± 0.02	5.85 ± 0.01	11.70 ± 0.01

<sup>a</sup> The visible absolute magnitude of the object from the Minor Planet Center. The values from the MPC differ from the R-band absolute magnitudes found for the few objects in which we have actual phase curves as shown in Table 3.

<sup>b</sup> Mean red magnitude of the object. For the four objects observed at significantly different phase angles the data near the lowest phase angle are used: Eris in 2005 October, Orcus in 2005 February, 90568 in 2005 March, and 120348 in 2005 October.

<sup>c</sup> Number of nights data were taken to determine the light curve.

<sup>d</sup> The peak-to-peak range of the light curve.

<sup>e</sup> The light-curve period if there is one maximum per period.

<sup>f</sup> The light-curve period if there are two maxima per period.

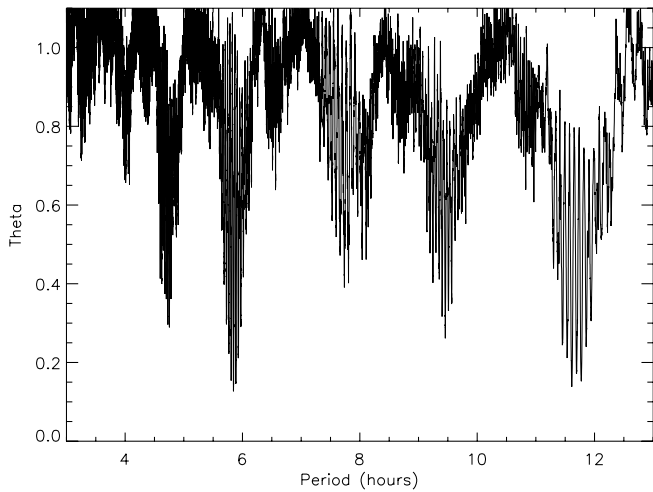


FIG. 1.—Phase dispersion minimization (PDM) plot for (120348) 2004 TY<sub>364</sub>. The best-fit single-peaked period is near 5.85 hr.

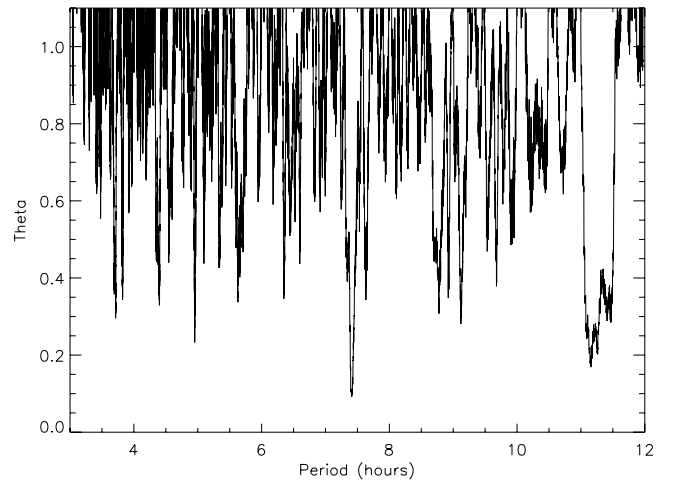


FIG. 4.—PDM plot for (84922) 2003 VS<sub>2</sub>. The best fit is the double-peaked period near 7.41 hr.

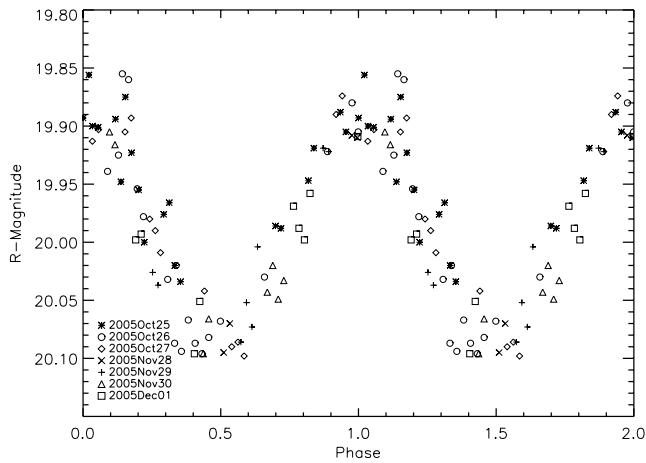


FIG. 2.—Phased best-fit single-peaked period for (120348) 2004 TY<sub>364</sub> of 5.85 hr. The peak-to-peak amplitude is about 0.22 mag. The data from November and December have been vertically shifted to correspond to the same phase angle as the data from October using the phase function found for this object in this work. Individual error bars for the measurements are not shown for clarity but are generally  $\pm 0.01$  mag, as seen in Table 1.

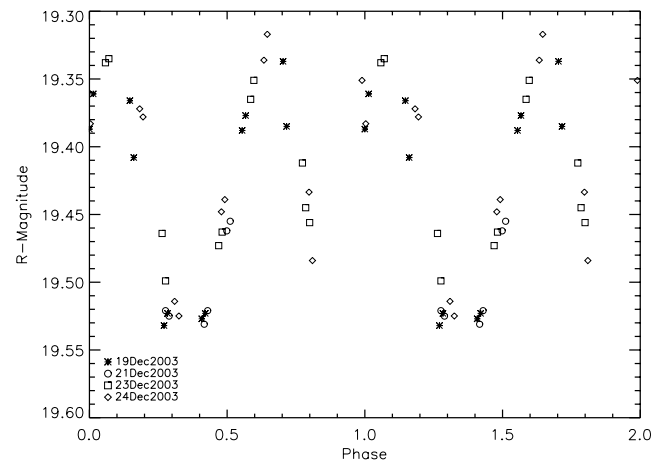


FIG. 5.—Phased best-fit double-peaked period for (84922) 2003 VS<sub>2</sub> of 7.41 hr. The peak-to-peak amplitude is about 0.21 mag. The two peaks have differences, since one is slightly wider while the other is slightly shorter in amplitude. This is the best-fit period for (84922) 2003 VS<sub>2</sub>. Individual error bars for the measurements are not shown for clarity but are generally  $\pm 0.01$  mag, as seen in Table 1.

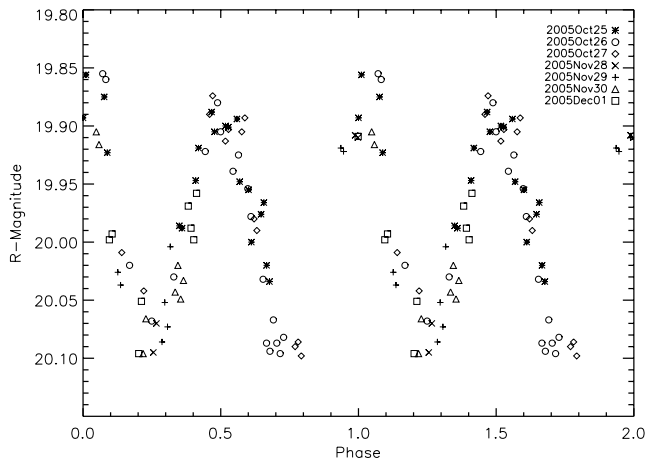


FIG. 3.—Phased double-peaked period for (120348) 2004 TY<sub>364</sub> of 11.70 hr. The data from November and December have been vertically shifted to correspond to the same phase angle as the data from October using the phase function found for this object in this work. Individual error bars for the measurements are not shown for clarity but are generally  $\pm 0.01$  mag, as seen in Table 1.

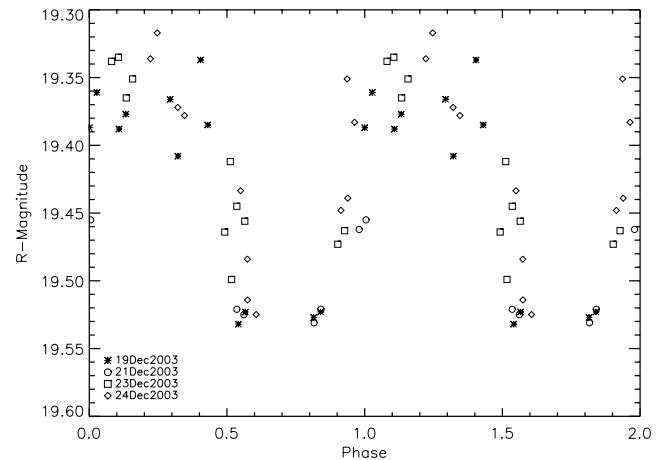


FIG. 6.—Phased single-peaked period for (84922) 2003 VS<sub>2</sub> of 3.70 hr. The single-peaked period for 2003 VS<sub>2</sub> does not look well matched and has a larger scatter about the solution compared to the double-peaked period shown in Fig. 5. Individual error bars for the measurements are not shown for clarity but are generally  $\pm 0.01$  mag, as seen in Table 1.

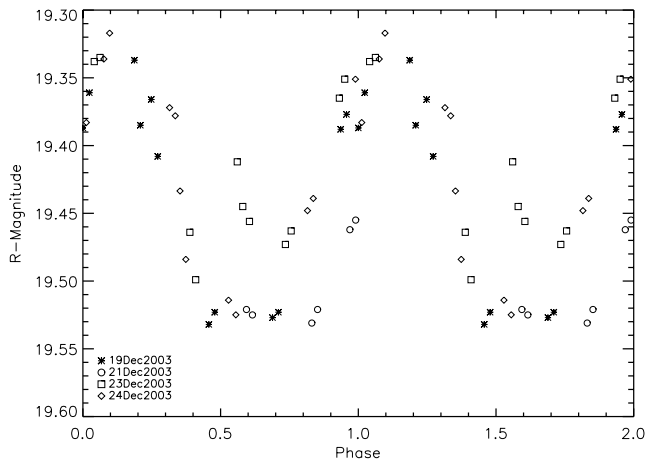


FIG. 7.—Phased single-peaked period for (84922) 2003 VS<sub>2</sub> of 4.39 hr. Again, the single-peaked period for 2003 VS<sub>2</sub> does not look well matched and has a larger scatter about the solution compared to the double-peaked period shown in Fig. 5. Individual error bars for the measurements are not shown for clarity but are generally  $\pm 0.01$  mag, as seen in Table 1.

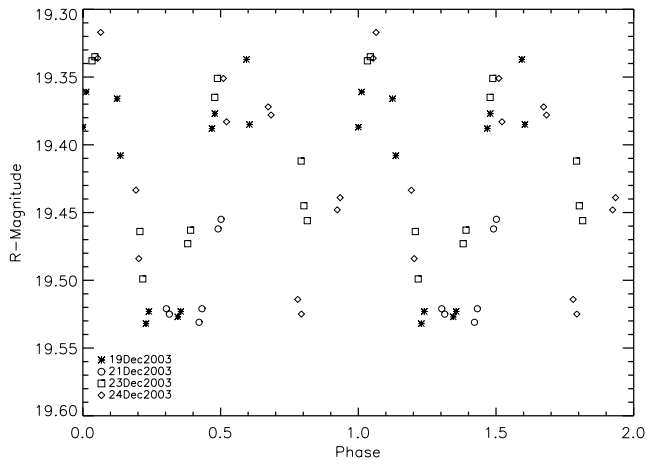


FIG. 8.—Phased double-peaked period for (84922) 2003 VS<sub>2</sub> of 8.77 hr. This double-peaked period for 2003 VS<sub>2</sub> does not look well matched and has a larger scatter about the solution compared to the 7.41 hr double-peaked period shown in Fig. 5. Individual error bars for the measurements are not shown for clarity but are generally  $\pm 0.01$  mag, as seen in Table 1.

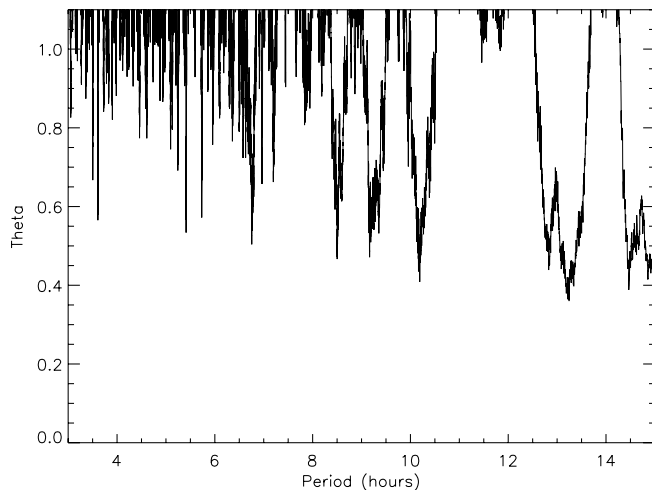


FIG. 9.—PDM plot for 2001 YH<sub>140</sub>. The best fit is the single-peaked period near 13.25 hr. The other possible fits near 8.5, 9.15, and 10.25 hr do not look good when phasing the data and viewing the result by eye.

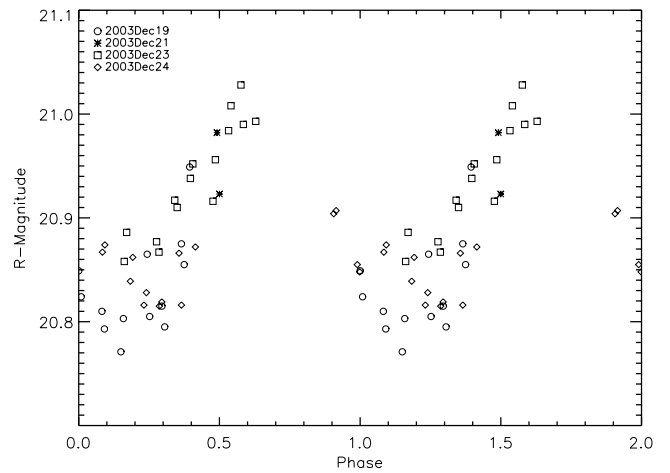


FIG. 10.—Phased best-fit single-peaked period for 2001 YH<sub>140</sub> of 13.25 hr. The peak-to-peak amplitude is about 0.21 mag. Individual error bars for the measurements are not shown for clarity but are generally  $\pm 0.02$  mag, as seen in Table 1.

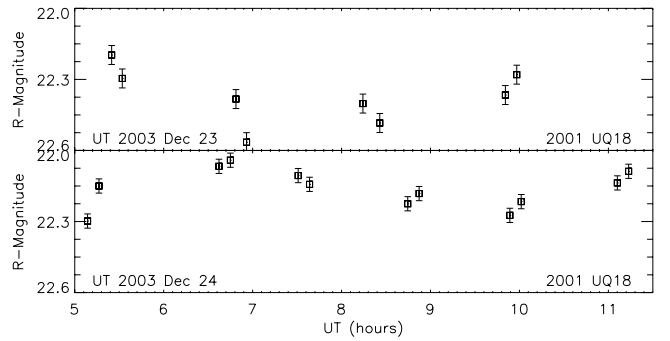


FIG. 11.—Flat light curve of (148780) 2001 UQ<sub>18</sub>. The KBO may have a significant amplitude light curve, but further observations are needed to confirm.

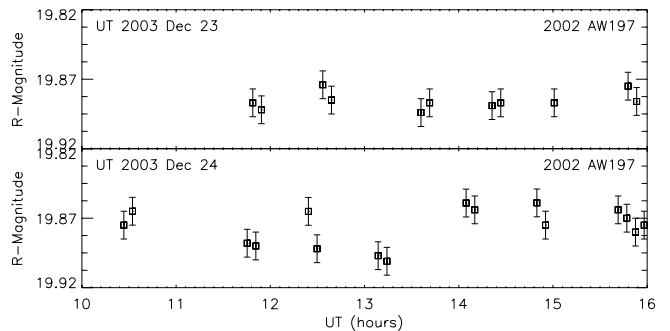


FIG. 12.—Flat light curve of (55565) 2002 AW<sub>197</sub>. The KBO has no significant short-term variations larger than 0.03 mag over 2 days.

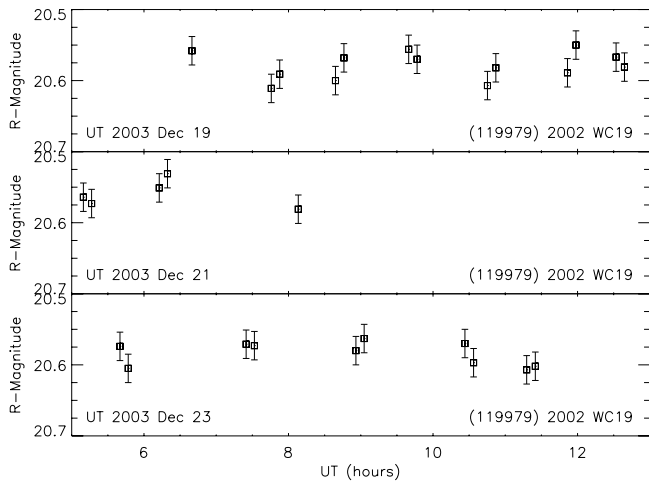


FIG. 13.—Flat light curve of (119979) 2002 WC<sub>19</sub>. The KBO has no significant short-term variations larger than 0.03 mag over 4 days. Additional data for 2002 WC<sub>19</sub> are shown in Fig. 14.

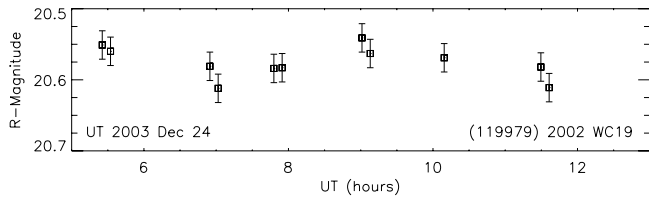


FIG. 14.—Flat light curve of (119979) 2002 WC<sub>19</sub>. The KBO has no significant short-term variations larger than 0.03 mag over 4 days. Additional data for 2002 WC<sub>19</sub> are shown in Fig. 13.

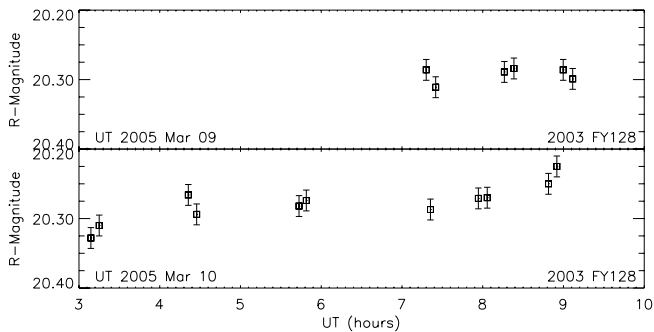


FIG. 15.—Flat light curve of (120132) 2003 FY<sub>128</sub>. The KBO has no significant short-term variations larger than 0.08 mag over 2 days.

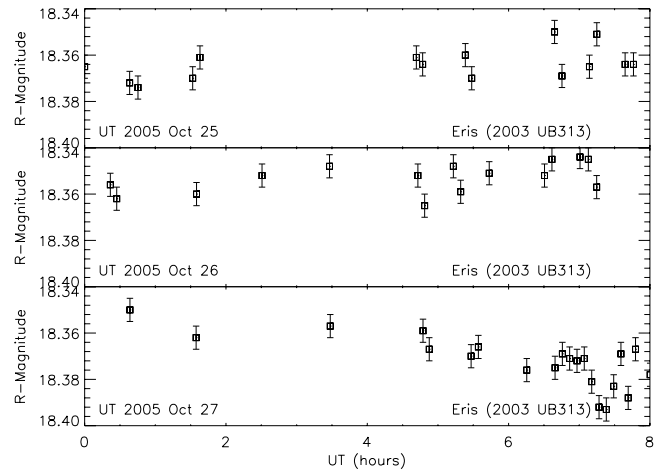


FIG. 16.—Flat light curve of Eris (2003 UB<sub>313</sub>) in 2005 October. The KBO has no significant short-term variations larger than 0.01 mag over several days. Additional data for Eris are shown in Fig. 17.

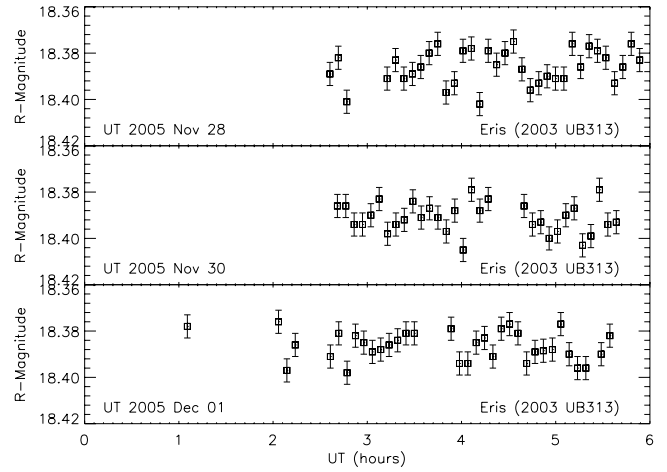


FIG. 17.—Flat light curve of Eris (2003 UB<sub>313</sub>) in 2005 November and December. The KBO has no significant short-term variations larger than 0.01 mag over several days. Data from November 29 are not plotted, since the Eris photometry is mildly contaminated by several nearby extended galaxies. Additional data for Eris are shown in Fig. 16.

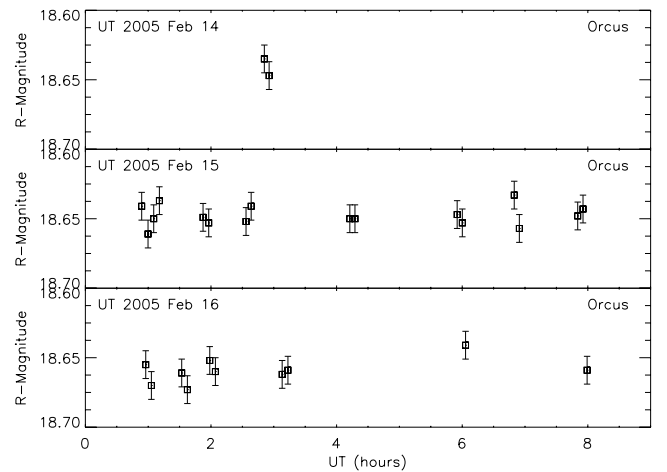


FIG. 18.—Flat light curve of (90482) Orcus 2004 DW in 2005 February. The KBO has no significant short-term variations larger than 0.03 mag over several days. Additional data for Orcus are shown in Fig. 19.

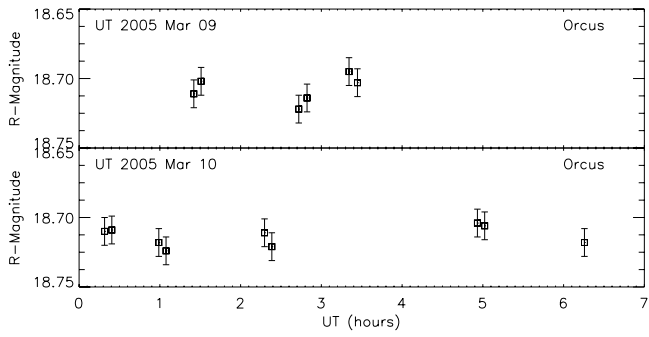


FIG. 19.—Flat light curve of (90482) Orcus 2004 DW in 2005 March. The KBO has no significant short-term variations larger than 0.03 mag over several days. Additional data for Orcus are shown in Fig. 18.

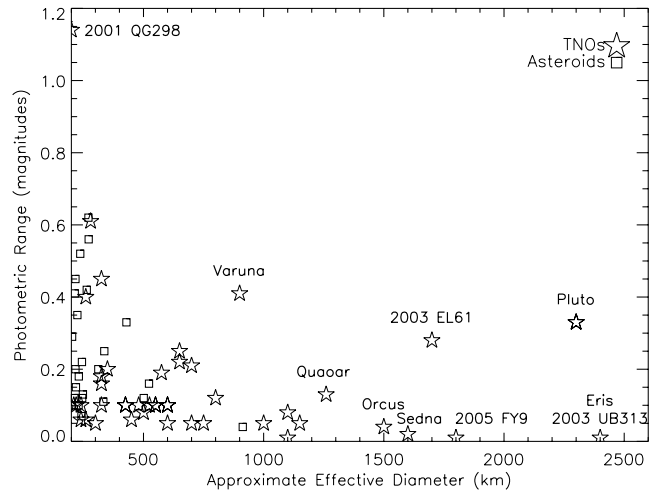


FIG. 22.—Diameter of asteroids and TNOs vs. their light-curve amplitudes. The TNO sizes if unknown are calculated assuming they have moderate albedos of about 10%. For objects with flat light curves they are plotted at the variation limit found by observations.

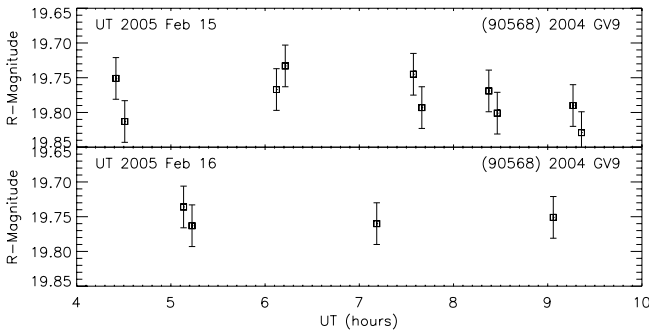


FIG. 20.—Flat light curve of (90568) 2004 GV<sub>9</sub> in 2005 February. The KBO has no significant short-term variations larger than 0.1 mag over several days. Additional data for 2004 GV<sub>9</sub> are shown in Fig. 21.

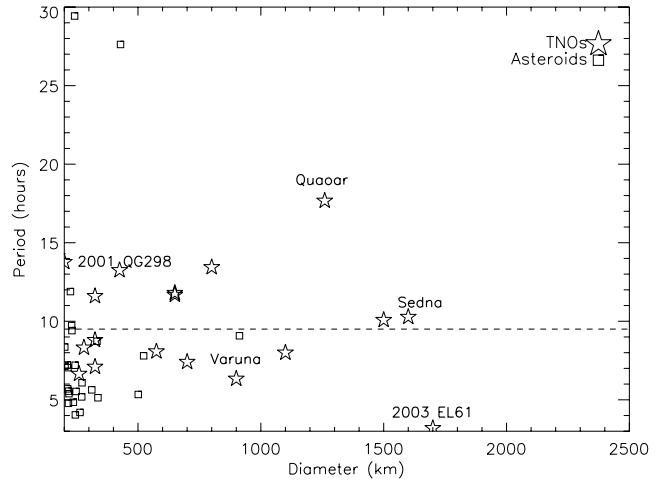


FIG. 23.—Same as Fig. 22, except the diameter vs. the light-curve period is plotted. The dashed line is the median of known TNO rotation periods ( $9.5 \pm 1$  hr), which is significantly above the median large MBA rotation periods ( $7.0 \pm 1$  hr). Pluto falls off the graph in the upper right corner because of its slow rotation created by the tidal locking to its satellite Charon.

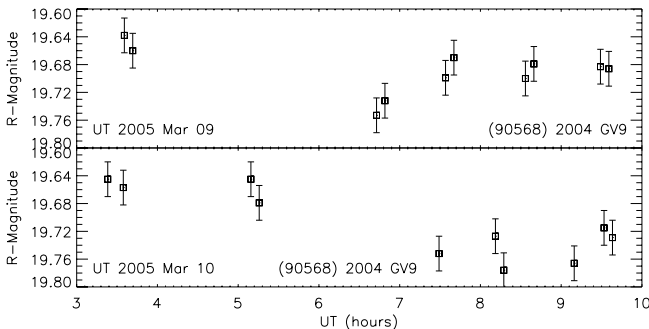


FIG. 21.—Flat light curve of (90568) 2004 GV<sub>9</sub> in 2005 March. The KBO has no significant short-term variations larger than 0.1 mag over several days. Additional data for 2004 GV<sub>9</sub> are shown in Fig. 20.

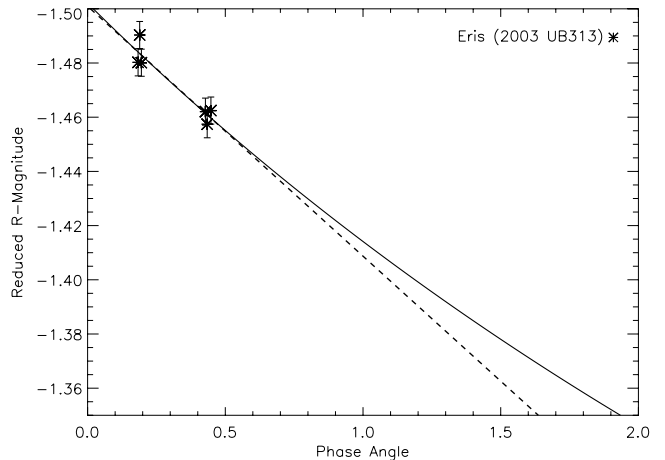


FIG. 24.—Phase curve for Eris (2003 UB<sub>313</sub>). The dashed line is the linear fit to the data, while the solid line uses the Bowell et al. (1989) H-G scattering formalism. In order to create only a few points with small error bars, the data have been averaged for each observing night.

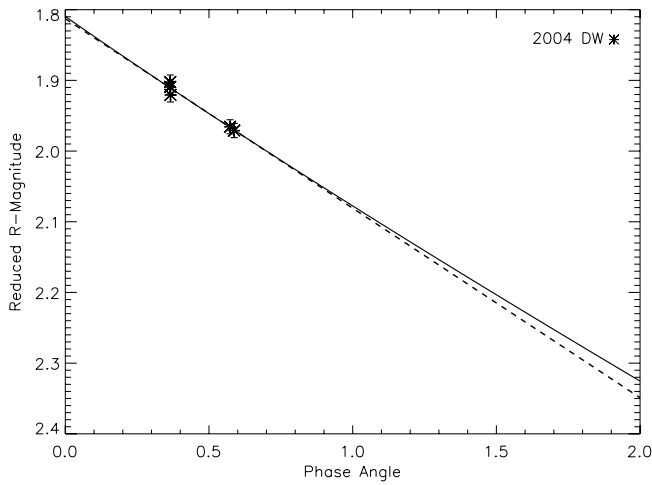


FIG. 25.—Same as Fig. 24, but for (90482) Orcus 2004 DW.

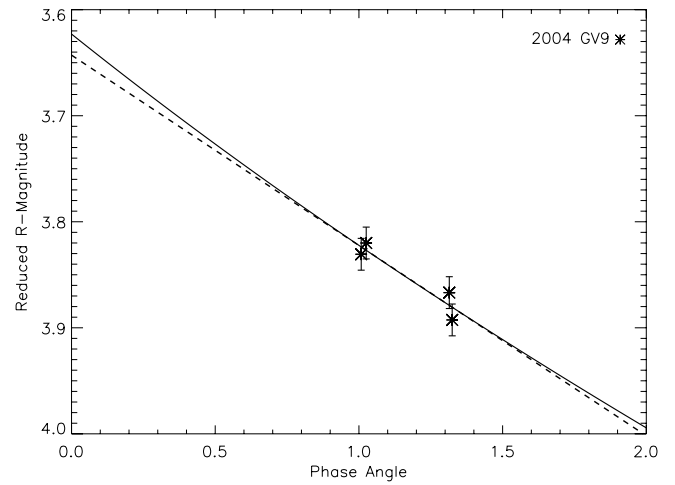


FIG. 27.—Same as Fig. 24, but for (90568) 2004 GV<sub>9</sub>.

within the small aperture used for the KBOs was corrected by determining the correction from the small to the large aperture using the point-spread function of the field stars. Second, I performed photometry on the KBOs using the same field stars but only using the large aperture on the KBOs. The smaller apertures allow better photometry for the fainter objects, since it uses only the high signal-to-noise ratio central pixels. The range of radii varies because the actual radii used depends on the seeing. The worse the seeing the larger the radius of the aperture needed in order to optimize the photometry. Both techniques found similar results, although, as expected, the smaller aperture gives less scatter for the fainter objects, while the larger aperture is superior for the brighter objects.

Photometric standard stars from Landolt (1992) were used for calibration. Each individual object was observed at all times in the same filter and with the same telescope setup. Relative photometric calibration from night to night was very stable, since the same field stars were observed. The few observations that were taken in mildly nonphotometric conditions (i.e., thin cirrus) were easily calibrated to observations of the same field stars on the photometric nights. Thus, the data points on these mildly nonphotometric nights are almost as good as the other data, with perhaps a slightly larger error bar. The dominate source of error in the photometry comes from simple root  $N$  noise.

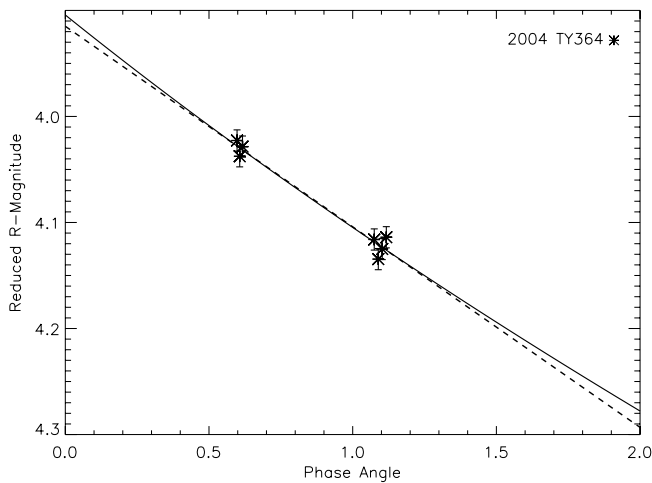


FIG. 26.—Same as Fig. 24, but for (120348) 2004 TY<sub>364</sub>.

### 3. LIGHT-CURVE CAUSES

The apparent magnitude or brightness of an atmosphereless inert body in our solar system is mainly from reflected sunlight and can be calculated as

$$m_R = m_{\odot} - 2.5 \log [p_R r^2 \phi(\alpha) / (2.25 \times 10^{16} R^2 \Delta^2)], \quad (1)$$

in which  $r$  (in km) is the radius of the KBO,  $R$  (in AU) is the heliocentric distance,  $\Delta$  (in AU) is the geocentric distance,  $m_{\odot}$  is the apparent red magnitude of the Sun ( $-27.1$ ),  $m_R$  is the apparent red magnitude,  $p_R$  is the red geometric albedo, and  $\phi(\alpha)$  is the phase function in which the phase angle  $\alpha = 0^\circ$  at opposition and  $\phi(0) = 1$ .

The apparent magnitude of the TNO may vary for the main following reasons:

1. The geometry in which  $R$ ,  $\Delta$ , and/or  $\alpha$  changes for the TNO. Geometrical considerations at the distances of the TNOs are usually only noticeable over a few weeks or longer and thus are considered long-term variations. These are further discussed in § 5.
2. The TNO's albedo,  $p_R$ , may not be uniform on its surface, causing the apparent magnitude to vary as the different albedo markings on the TNOs surface rotate in and out of our line of sight. Albedo or surface variations on an object usually cause less than a 30% difference from maximum to minimum brightness of an object. (134340) Pluto, because of its atmosphere (Spencer et al. 1997), has one of the highest known amplitudes from albedo variations ( $\sim 0.3$  mag; Buie et al. 1997).
3. Shape variations or elongation of an object will cause the effective radius of an object to our line of sight to change as the TNO rotates. A double-peaked periodic light curve is expected to be seen in this case, since the projected cross section would go between two minima (short axis) and two maxima (long axis) during one complete rotation of the TNO. Elongation from material strength is likely for small TNOs ( $r < 100$  km), but for the larger TNOs observed in this paper no significant elongation is expected from material strength because of their large self-gravity.

A large TNO ( $r > 100$  km) may be significantly elongated if it has a large amount of rotational angular momentum. An object will be near breakup if it has a rotation period near the critical rotation period ( $P_{\text{crit}}$ ) at which centripetal acceleration

TABLE 3  
PHASE FUNCTION DATA FOR KBOs

Name	$m_R(1, 1, 0)^a$ (mag)	$H^b$ (mag)	MPC <sup>c</sup> (mag)	$\beta(\alpha < 2^\circ)^d$ (mag deg <sup>-1</sup> )
(136199) Eris 2003 UB <sub>313</sub> .....	$-1.50 \pm 0.02$	$-1.50 \pm 0.02$	-1.65	$0.09 \pm 0.03$
(90482) Orcus 2004 DW.....	$1.81 \pm 0.05$	$1.81 \pm 0.05$	1.93	$0.26 \pm 0.05$
(90568) 2004 GV <sub>9</sub> .....	$3.64 \pm 0.06$	$3.62 \pm 0.06$	3.5	$0.18 \pm 0.06$
(120348) 2004 TY <sub>364</sub> .....	$3.91 \pm 0.03$	$3.90 \pm 0.03$	4.0	$0.19 \pm 0.03$

<sup>a</sup> The *R*-band reduced magnitude determined from the linear phase coefficient found in this work.

<sup>b</sup> The *R*-band absolute magnitude determined as described in *Bowell et al. (1989)*.

<sup>c</sup> The *R*-band absolute magnitude from the Minor Planet Center converted from the *V* band as shown in Table 2 to the *R* band using the known colors of the objects:  $V - R = 0.45$  for Eris (*Brown et al. 2005*),  $V - R = 0.37$  for Orcus (*de Bergh et al. 2005*), and a nominal value of  $V - R = 0.5$  for 90568 and 120348, since these objects do not have known  $V - R$  colors.

<sup>d</sup>  $\beta(\alpha < 2^\circ)$  is the phase coefficient in magnitudes per degree at phase angles  $< 2^\circ$ .

equals gravitational acceleration toward the center of a rotating spherical object,

$$P_{\text{crit}} = \left( \frac{3\pi}{G\rho} \right)^{1/2}, \quad (2)$$

where  $G$  is the gravitational constant and  $\rho$  is the density of the object. With  $\rho = 10^3 \text{ kg m}^{-3}$  the critical period is about 3.3 hr. At periods just below the critical period the object will likely break apart. For objects with rotations significantly above the critical period the shapes will be bimodal Maclaurin spheroids which do not show any significant rotational light curves produced by shape (*Jewitt & Sheppard 2002*). For periods just above the critical period the equilibrium figures are triaxial ellipsoids which are elongated from the large centripetal force and usually show prominent rotational light curves (*Weidenschilling 1981; Holsapple 2001; Jewitt & Sheppard 2002*).

For an object that is triaxially elongated the peak-to-peak amplitude of the rotational light curve allows for the determination of the projection of the body shape into the plane of the sky by (*Binzel et al. 1989*)

$$\Delta m = 2.5 \log \left( \frac{a}{b} \right) - 1.25 \log \left( \frac{a^2 \cos^2 \theta + c^2 \sin^2 \theta}{b^2 \cos^2 \theta + c^2 \sin^2 \theta} \right), \quad (3)$$

where  $a \geq b \geq c$  are the semiaxes with the object in rotation about the  $c$  axis,  $\Delta m$  is expressed in magnitudes, and  $\theta$  is the angle at which the rotation ( $c$ ) axis is inclined to the line of sight (an object with  $\theta = 90^\circ$  is viewed equatorially). The amplitudes of the light curves produced from rotational elongation can range up to about 0.9 mag (*Leone et al. 1984*).

Assuming  $\theta = 90^\circ$  gives  $a/b = 10^{0.4\Delta m}$ . Thus, the easily measured quantities of the rotation period and amplitude can be used to determine a minimum density for an object if it is assumed to be rotationally elongated and strengthless (i.e., the bodies structure behaves like a fluid; *Chandrasekhar 1969*). The two best cases of this high angular momentum elongation in the Kuiper Belt are (20000) Varuna (*Jewitt & Sheppard 2002*) and (136108) 2003 EL<sub>61</sub> (*Rabinowitz et al. 2006*).

4. Periodic light curves may be produced if a TNO is an eclipsing or contact binary. A double-peaked light curve would be expected, with a possible characteristic notch shape near the minimum of the light curve. Because the two objects may be tidally elongated the light curves can range up to about 1.2 mag (*Leone et al. 1984*). The best example of such an object in the Kuiper Belt is 2001 QG<sub>298</sub> (*Sheppard & Jewitt 2004*).

5. A nonperiodic short-term light curve may occur from a complex rotational state, a recent collision, a binary with each component having a large light-curve amplitude and a different rotation period, or outgassing/cometary activity. These types of short-term variability are expected to be extremely rare and none have yet been reliably detected in the Kuiper Belt (*Sheppard & Jewitt 2003; Belskaya et al. 2006*).

#### 4. LIGHT-CURVE RESULTS AND ANALYSIS

The photometric measurements for the 10 newly observed KBOs are listed in Table 1, where the columns include the start time of each integration, the corresponding Julian date, and the magnitude. No correction for light travel time has been made. Results of the light-curve analysis for all the KBOs newly observed are summarized in Table 2.

The phase dispersion minimization (PDM) method (*Stellingwerf 1978*) was used to search for periodicity in the individual light curves. In PDM, the metric is the so-called Theta parameter, which is essentially the variance of the unphased data divided by the variance of the data when phased by a given period. The best-fit period should have a very small dispersion compared to the unphased data, and thus Theta  $\ll 1$  indicates that a good fit has been found. In practice, a Theta of less than 0.4 indicates a possible periodic signature.

##### 4.1. (120348) 2004 TY<sub>364</sub>

Through the PDM analysis I found a strong Theta minima for 2004 TY<sub>364</sub> near a period of  $P = 5.85$  hr, with weaker alias periods flanking this (Fig. 1). Phasing the data to all possible periods in the PDM plot with Theta  $< 0.4$  found that only the single-peaked period near 5.85 hr and the double-peaked period near 11.70 hr fit all the data obtained from 2005 October, November, and December. Both periods have an equally low Theta parameter of about 0.15 and either could be the true rotation period (Figs. 2 and 3). The peak-to-peak amplitude is  $0.22 \pm 0.02$  mag.

If 2004 TY<sub>364</sub> has a double-peaked period, it may be elongated from its high angular momentum. If the TNO is assumed to be observed equator on then from equation (3) the  $a:b$  axis ratio is about 1.2. Following *Jewitt & Sheppard (2002)* I assume that the TNO is a rotationally elongated strengthless rubble pile. Using the spin period of 11.7 hr, the 1.2  $a:b$  axis ratio found above and the Jacobi ellipsoid tables produced by *Chandrasekhar (1969)*, I find that the minimum density of 2004 TY<sub>364</sub> is about  $290 \text{ kg m}^{-3}$  with an  $a : c$  axis ratio of about 1.9. This density is quite low, which leads one to believe either that the TNO is

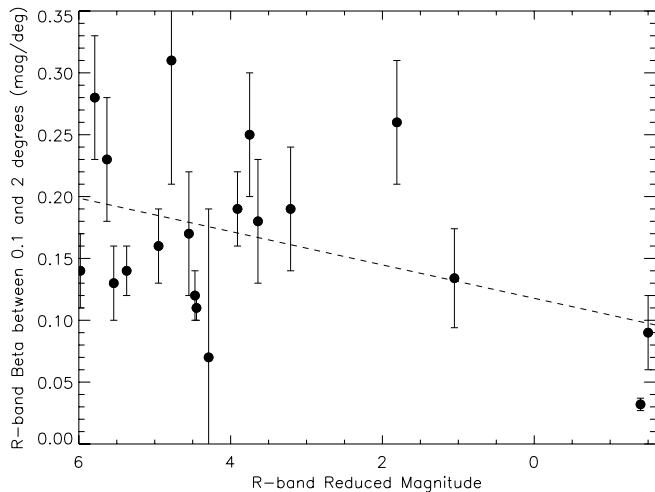


FIG. 28.— $R$ -band reduced magnitude vs. the  $R$ -band linear phase coefficient  $\beta$  ( $\alpha < 2^\circ$ ) for TNOs. The  $R$ -band data are from this work and Sheppard & Jewitt (2002, 2003), as well as Sedna from Rabinowitz et al. (2007) and Pluto from Buratti et al. (2003). A linear fit is shown by the dashed line. Larger objects (smaller reduced magnitudes) may have smaller  $\beta$  at the 97% confidence level using the Pearson correlation coefficient.

not being viewed equator-on, or that the relatively long double-peaked period is not created from high angular momentum of the object.

#### 4.2. (84922) 2003 VS<sub>2</sub>

The KBO 2003 VS<sub>2</sub> has a very low Theta of less than 0.1 near 7.41 hr in the PDM plot (Fig. 4). Phasing the 2003 December data to this period shows a well-defined double-peaked period (Fig. 5). The single-peaked period for this result would be near 3.71 hr, which was a possible period determined for this object by Ortiz et al. (2006). The 3.71 hr single-peaked period does not look as convincing (Fig. 6), which confirms the PDM result that the single-peaked period has about 3 times more dispersion than the double-peaked period. This is likely because one of the peaks is taller in amplitude ( $\sim 0.05$  mag) and a little wider. The other single-peaked period of 4.39 hr (Fig. 7) and the double-peaked period of 8.77 hr (Fig. 8) mentioned by Ortiz et al. (2006) do not show a low Theta in the PDM and also do not look convincing when examining the phased data. The peak-to-peak amplitude is  $0.21 \pm 0.02$  mag, which is similar to that detected by Ortiz et al. (2006).

The fast rotation of 7.41 hr and its double-peaked nature suggests that 2003 VS<sub>2</sub> may be elongated from its high angular momentum. Using equation (3) and assuming that the TNO is observed equator-on, the  $a:b$  axis ratio is about 1.2. Using the spin period of 7.41 hr, the 1.2  $a:b$  axis ratio and the Jacobi ellipsoid tables produced by Chandrasekhar (1969), I find the minimum density of 2003 VS<sub>2</sub> is about  $720 \text{ kg m}^{-3}$  with an  $a:c$  axis ratio of about 1.9. This result is similar to other TNO densities found through the Jacobian Ellipsoid assumption (Jewitt & Sheppard 2002; Sheppard & Jewitt 2002; Rabinowitz et al. 2006), as well as recent thermal results from the *Spitzer Space Telescope* (Stansberry et al. 2006).

#### 4.3. (126154) 2001 YH<sub>140</sub>

(126154) 2001 YH<sub>140</sub> shows variability of  $0.21 \pm 0.04$  mag. The PDM for this TNO shows possible periods near 8.5, 9.15, 10.25, and 13.25 hr, although only the 13.25 hr period has a Theta less than 0.4 (Fig. 9). Visibly examining the phased data

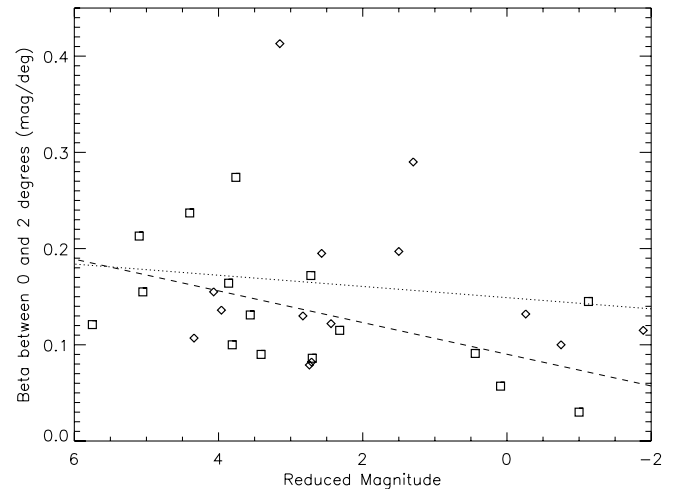


FIG. 29.—Same as Fig. 28 except for the  $V$  band (squares) and  $I$  band (diamonds). Pluto and Charon data are from Buie et al. (1997), and the other data are from Rabinowitz et al. (2007). Error bars are usually less than  $0.04 \text{ mag deg}^{-1}$ . The  $V$ -band data show a similar correlation (97% confidence, dashed line) as found for the  $R$ -band data in Fig. 28, that is, larger objects may have smaller  $\beta$ . There is no correlation found using the  $I$ -band data (dotted line).

finds only the 13.25 hr period is viable (Fig. 10). This is consistent with the observation that one minimum and one maximum were shown on 2003 December 23 in about six and a half hours, which would give a single-peaked light curve of twice this time or about 13.25 hr. Ortiz et al. (2006) found this object to have a similar variability but with very limited data could not obtain a reliable period. Ortiz et al. did have one period of 12.99 hr, which may be consistent with our result.

#### 4.4. Flat Rotation Curves

Seven of the 10 newly observed KBOs—(148780) 2001 UQ<sub>18</sub>, (55565) 2002 AW<sub>197</sub>, (119979) 2002 WC<sub>19</sub>, (120132) 2003 FY<sub>128</sub>, (136199) Eris 2003 UB<sub>313</sub>, (90482) Orcus 2004 DW, and (90568) 2004 GV<sub>9</sub>—showed no variability within the photometric uncertainties of the observations (Table 2; Figs. 11–21). These KBOs thus either have extremely long rotational periods, are viewed nearly pole-on, or most likely have small peak-to-peak rotational amplitudes. The upper limits for the objects' short-term rotational variability as shown in Table 2 were determined through a Monte Carlo simulation. The Monte Carlo simulation determined the lowest possible amplitude that would be seen in the data from the time sampling and variance of the photometry, as well as the errors on the individual points.

Ortiz et al. (2006) reported a possible  $0.04 \pm 0.02$  photometric range for (90482) Orcus 2004 DW and a period near 10 hr. I do not confirm this result here. Ortiz et al. (2006) also reported a marginal  $0.08 \pm 0.03$  photometric range for (55565) 2002 AW<sub>197</sub> with no one clear best period. I cannot confirm this result and find that for 2002 AW<sub>197</sub> the rotational variability appears significantly less than 0.08 mag.

Some of the KBOs in this sample appear to have a variability which is just below the threshold of the data detection, and thus no significant period could be obtained with the current data. In particular, 2001 UQ<sub>18</sub> appears to have a light curve with a significant amplitude above 0.1 mag, but the data are sparser for this object than most the others, and thus no significant period is found. Follow-up observations will be required in order to determine whether most of these flat light curve objects do have any significant short-term variability.

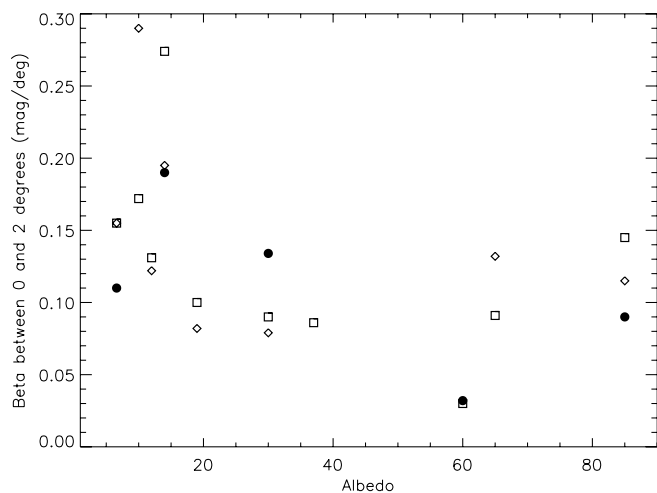


FIG. 30.—Same as Figs. 28 and 29, but showing the albedo vs. linear phase coefficient for TNOs. Filled circles represent *R*-band data, squares represent *I*-band data, and diamonds represent *L*-band data. Albedos are from Cruikshank et al. (2006).

#### 4.5. Comparisons with Size, Amplitude, Period, and MBAs

In Figures 22 and 23 are plotted the diameters of the largest TNOs and MBAs versus rotational amplitude and period, respectively. Most outliers on Figure 22 can easily be explained from the discussion in § 3. Varuna, 2003 EL<sub>61</sub>, and the other unmarked TNOs with photometric ranges above about 0.4 mag are all spinning faster than about 8 hr. They are thus likely hydrostatic equilibrium triaxial Jacobian ellipsoids which are elongated from their rotational angular momentum (Jewitt & Sheppard 2002; Sheppard & Jewitt 2002; Rabinowitz et al. 2006). 2001 QG<sub>298</sub>'s large photometric range is probably because this object is a contact binary indicative of its longer period and notched shaped light curve (Sheppard & Jewitt 2004). Pluto's relatively large amplitude light curve is best explained through its active atmosphere (Spencer et al. 1997). Like the MBAs, the photometric amplitudes of the TNOs start to increase significantly at sizes less than about 300 km in diameter. The likely reason is that this size range is where the objects are still large enough to be dominated by self-gravity and are not easily disrupted through collisions but can still have their angular momentum highly altered from the collisional process (Farinella & Paolicchi 1982; Davis & Farinella 1997). Thus, this is the region most likely to be populated by high angular momentum triaxial Jacobian ellipsoids (Farinella et al. 1992).

From this work Eris (2003 UB<sub>313</sub>) has one of the highest signal-to-noise ratio time-resolved photometry measurements of any TNO searched for a rotational period. There is no obvious rotational light curve larger than about 0.01 mag in our extensive data, which indicates a very uniform surface, a rotation period of over a few days, or a pole-on viewing geometry. Carraro et al. (2006) suggest a possible 0.05 mag variability for Eris between nights, but this is not obvious in this data set. The similar inferred composition and size of Eris to Pluto suggests these objects should behave in a very similar manner (Brown et al. 2005, 2006). Since Pluto has a relatively substantial atmosphere at its current position of about 30 AU (Elliot et al. 2003; Sicardy et al. 2003), it is very likely that Eris has an active atmosphere when near its perihelion of 38 AU. At Eris' current distance of 97 AU its surface thermal temperature should be over 20° colder than when at perihelion. Like Pluto, Eris' putative atmosphere near perihelion would likely be composed of N<sub>2</sub>, CH<sub>4</sub>, or CO,

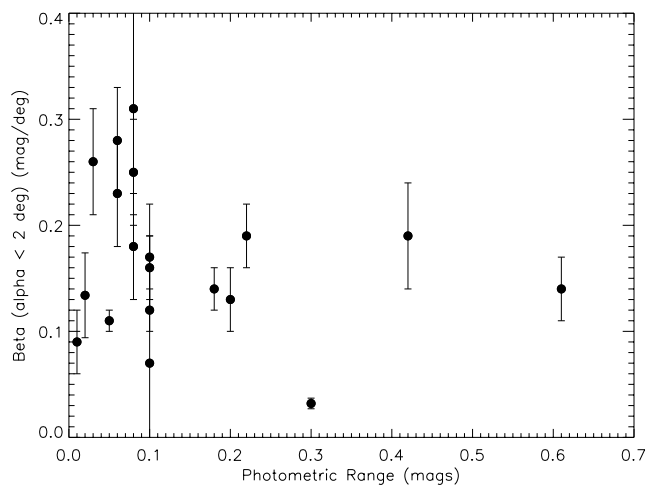


FIG. 31.—Same as Fig. 28, but showing the light-curve amplitude vs. the linear phase coefficient for TNOs. TNOs with no measured rotational variability are plotted with their possible amplitude upper limits. No significant correlation is found.

which would mostly condense when near aphelion (Spencer et al. 1997; Hubbard 2003), effectively resurfacing the TNO every few hundred years. This is the most likely explanation as to why the surface of Eris appears so uniform. This may also be true for 2005 FY<sub>9</sub>, which appears compositionally similar to Pluto (Licandro et al. 2006) and at 52 AU is about 15° colder than Pluto.

Figure 23 shows that the median rotation period distribution for TNOs is about  $9.5 \pm 1$  hr, which is marginally larger than for similarly sized MBAs ( $7.0 \pm 1$  hr; Sheppard & Jewitt 2002; Lacerda & Luu 2006). If confirmed, the likely reasons for this difference are the collisional histories of each reservoir, as well as the objects' compositions.

## 5. PHASE-CURVE RESULTS

The phase function of an object's surface mostly depends on the albedo, texture, and particle structure of the regolith. Four of the newly imaged TNOs [Eris 2003 UB<sub>313</sub>, (120348) 2004 TY<sub>364</sub>, Orcus 2004 DW, and (90568) 2004 GV<sub>9</sub>] were viewed on two separate telescope observing runs occurring at significantly different phase angles (Figs. 24–27). This allowed their linear phase functions,

$$\phi(\alpha) = 10^{-0.4\beta\alpha}, \quad (4)$$

to be estimated where  $\alpha$  is the phase angle in degrees and  $\beta$  is the linear phase coefficient in magnitudes per degree (Table 3). The phase angles for TNOs are always less than about 2° as seen from the Earth. Most atmosphereless bodies show opposition effects at such small phase angles (Muinonen et al. 2002). The TNOs appear to have mostly linear phase curves between phase angles of about 2° and 0.1° (Sheppard & Jewitt 2002, 2003; Rabinowitz et al. 2007). For phase angles smaller than about 0.1° TNOs may display an opposition spike (Hicks et al. 2005; Belskaya et al. 2006).

The moderate to large KBOs Orcus, 2004 TY<sub>364</sub>, and 2004 GV<sub>9</sub> show steep linear *R*-band phase slopes (0.18–0.26 mag deg<sup>-1</sup>) similar to previous measurements of similarly sized moderate to large TNOs (Sheppard & Jewitt 2002, 2003; Rabinowitz et al. 2007). In contrast, the extremely large dwarf planet Eris (2003 UB<sub>313</sub>) has a shallower phase slope (0.09 mag deg<sup>-1</sup>)

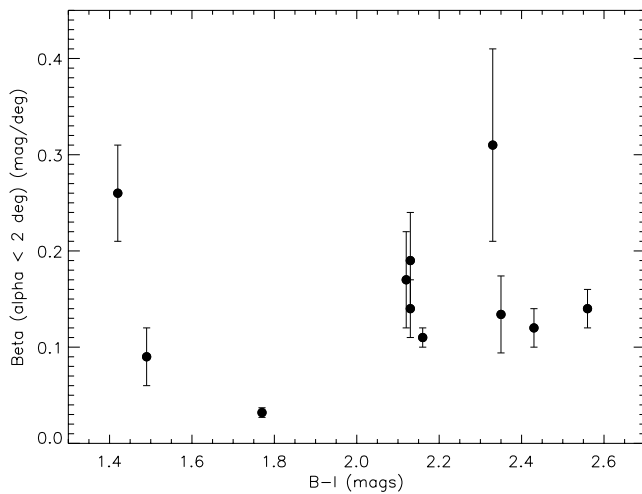


FIG. 32.—Same as Fig. 28, but showing the  $B - I$  broadband colors vs. the linear phase coefficient for TNOs. Colors are from Barucci et al. (2005). No significant correlation is found.

more similar to Charon ( $\sim 0.09 \text{ mag deg}^{-1}$ ; Buie et al. 1997) and possibly Pluto ( $\sim 0.03 \text{ mag deg}^{-1}$ ; Buratti et al. 2003). Empirically lower phase coefficients between  $0.5^\circ$  and  $2^\circ$  may correspond to bright icy objects whose surfaces have probably been recently resurfaced such as Triton, Pluto, and Europa (Buie et al. 1997; Buratti et al. 2003; Rabinowitz et al. 2007). Thus, Eris' low  $\beta$  is consistent with it having an icy surface that has recently been resurfaced.

In Figures 28–32 are plotted the linear phase coefficients found for several TNOs versus several different parameters (reduced magnitude, albedo, rotational photometric amplitude, and  $B - I$  broadband color). Table 4 shows the significance of any correlations. Based on only a few large objects it appears that the larger TNOs may have lower  $\beta$  values. This is true for the  $R$ -band and  $V$ -band data at the 97% confidence level, but, interestingly, using data from Rabinowitz et al. (2007) no correlation is seen in the  $I$  band (Table 4). Thus, further measurements are needed to determine whether there is a significantly strong correlation between the size and phase function of TNOs. Furthermore, it may be that the albedos are anticorrelated with  $\beta$ , but since we have such a small number of albedos known the statistics do not give good confidence in this correlation. If confirmed with additional observations, these correlations may be an indication that larger TNOs' surfaces are less susceptible to phase angle opposition effects at optical wavelengths. This could be because the larger TNOs have different surface properties from smaller TNOs due to active atmospheres, stronger self-gravity, or different surface layers from possible differentiation.

### 5.1. Absolute Magnitudes

From the linear phase coefficient the reduced magnitude,  $m_R(1, 1, 0) = m_R - 5 \log(R\Delta)$  or absolute magnitude  $H$  (Bowell et al. 1989), which is the magnitude of an object if it could be observed at heliocentric and geocentric distances of 1 AU and a phase angle of  $0^\circ$ , can be estimated (see Sheppard & Jewitt 2002 for further details). The results for  $m_R(1, 1, 0)$  and  $H$  are found to be consistent to within a couple hundredths of a magnitude (Table 3 and Figs. 24–27). It is found that the  $R$  band empirically determined absolute magnitudes of individual TNOs appears to be a few tenths of a magnitude different than what is given by the Minor Planet Center (MPC; Table 3). This is likely because the MPC assumes a generic phase function and color for

TABLE 4  
PHASE FUNCTION CORRELATIONS

$\beta$ vs. <sup>a</sup>	$r_{\text{corr}}$ <sup>b</sup>	$N$ <sup>c</sup>	Sig <sup>d</sup>
$m_R(1, 1, 0)$ .....	0.50	19	97%
$m_V(1, 1, 0)$ .....	0.54	16	97%
$m_I(1, 1, 0)$ .....	0.12	14	<60%
$p_R$ .....	-0.51	5	65%
$p_V$ .....	-0.38	9	70%
$p_I$ .....	-0.27	10	<60%
$\Delta m$ .....	-0.21	19	<60%
$B - I$ .....	-0.20	11	<60%

<sup>a</sup>  $\beta$  is the linear phase coefficient in magnitudes per degree at phase angles  $< 2^\circ$ . In this column we show what  $\beta$  is compared with to see whether there is any correlation;  $m_R(1, 1, 0)$ ,  $m_V(1, 1, 0)$ , and  $m_I(1, 1, 0)$  are the reduced magnitudes in the  $R$ ,  $V$ , and  $I$  bands, respectively, and are compared to the value of  $\beta$  determined at the same wavelength;  $p_R$ ,  $p_V$ , and  $p_I$  are the geometric albedos compared to  $\beta$  in the  $R$ ,  $V$ , and  $I$  bands, respectively;  $\Delta m$  is the peak-to-peak amplitude of the rotational light curve; and  $B - I$  is the color. The phase curves in the  $R$  band are from this work and Sheppard & Jewitt (2002, 2003), while the  $V$ - and  $I$ -band data are from Buie et al. (1997) and Rabinowitz et al. (2007). The albedo information is from Cruikshank et al. (2006) and the colors from Barucci et al. (2005).

<sup>b</sup>  $r_{\text{corr}}$  is the Pearson correlation coefficient.

<sup>c</sup>  $N$  is the number of TNOs used for the correlation.

<sup>d</sup> Sig is the confidence of significance of the correlation.

all TNOs, while these two physical properties appear to be significantly different for individual KBOs (Jewitt & Luu 1998). The work by Romanishin & Tegler (2005) attempts to determine various absolute magnitudes of TNOs by using MBA-type phase curves which are not appropriate for TNOs (Sheppard & Jewitt 2002).

## 6. SUMMARY

Ten large trans-Neptunian objects were observed in the  $R$  band to determine photometric variability on times scales of hours, days and months.

1. Three of the TNOs show obvious short-term photometric variability which is taken to correspond to their rotational states.

a) (120348) 2004 TY<sub>364</sub> shows a double-peaked period of 11.7 hr and if single-peaked is 5.85 hr. The peak-to-peak amplitude of the light curve is  $0.22 \pm 0.02 \text{ mag}$ .

b) (84922) 2003 VS<sub>2</sub> has a well-defined double-peaked period of 7.41 hr with a peak-to-peak amplitude of  $0.21 \pm 0.02 \text{ mag}$ . If the light curve is from elongation than 2003 VS<sub>2</sub>'s  $a:b$  axis ratio is at least 1.2 and the  $a:c$  axis ratio is about 1.9. Assuming that 2003 VS<sub>2</sub> is elongated from its high angular momentum and is a strengthless rubble pile it would have a minimum density of about  $720 \text{ kg m}^{-3}$ .

c) (126154) 2001 YH<sub>140</sub> has a single-peaked period of about 13.25 hr with a photometric range of  $0.21 \pm 0.04 \text{ mag}$ .

2. Seven of the TNOs show no short-term photometric variability within the measurement uncertainties.

a) Photometric measurements of the large TNOs (90482) Orcus and (55565) 2002 AW<sub>197</sub> showed no variability within or uncertainties. Thus, these measurements do not confirm possible small photometric variability found for these TNOs by Ortiz et al. (2006).

b) No short-term photometric variability was found for (136199) Eris 2003 UB<sub>313</sub> to about the 0.01 mag level. This high signal-to-noise ratio photometry suggests Eris is nearly spherical with a very uniform surface. Such a nearly uniform surface may

be explained by an atmosphere which is frozen onto the surface of Eris when near aphelion. The atmosphere, like Pluto's, may become active when near perihelion, effectively resurfacing Eris every few hundred years. The methane-rich TNO 2005 FY<sub>9</sub> may also be in a similar situation.

3. Four of the TNOs were observed over significantly different phase angles allowing their long-term photometric variability to be measured between phase angles of 0.1° and 1.5°.

a) TNOs Orcus, 2004 TY<sub>364</sub>, and 2004 GV<sub>9</sub> show steep linear *R*-band phase slopes between 0.18 and 0.26 mag deg<sup>-1</sup>.

b) Eris 2003 UB<sub>313</sub> shows a shallower *R*-band phase slope of 0.09 mag deg<sup>-1</sup>. This is consistent with Eris having a high-albedo, icy surface which may have recently been resurfaced.

c) At the 97% confidence level the largest TNOs have shallower *R*-band linear phase slopes compared to smaller TNOs. The largest TNOs surfaces may differ from the smaller TNOs because of their more volatile ice inventory, increased self-

gravity, active atmospheres, differentiation process, or collisional history.

4. The absolute magnitudes determined for a few TNOs through measuring their phase curves show a difference of several tenths of a magnitude from the Minor Planet Center values.

a) The values found for the reduced magnitude,  $m_R(1, 1, 0)$ , and absolute magnitude,  $H$ , are similar to within a few hundredths of a magnitude for most TNOs.

Support for this work was provided by NASA through Hubble Fellowship grant HF-01178.01-A awarded by the Space Telescope Science Institute, which is operated by the Association of Universities for Research in Astronomy, Inc., for NASA, under contract NAS5-26555. Observations at the UH telescope were supported by a grant to D. Jewitt from the NASA Planetary Astronomy Program.

#### REFERENCES

- Barucci, M., Belskaya, I., Fulchignoni, M., & Birlan, M. 2005, *AJ*, 130, 1291  
 Belskaya, I., Ortiz, J., Rousselot, P., Ivanova, V., Borisov, G., Shevchenko, V., & Peixinho, N. 2006, *Icarus*, 184, 277  
 Bertoldi, F., Altenhoff, W., Weiss, A., Menten, K., & Thum, C. 2006, *Nature*, 439, 563  
 Binzel, R., Farinella, P., Zappala, V., & Cellino, A. 1989, in *Asteroids II*, ed. R. Binzel, T. Gehrels, & M. Matthews (Tucson: Univ. Arizona Press), 416  
 Bowell, E., Hapke, B., Domingue, D., Lumme, K., Peltoniemi, J., & Harris, A. 1989, in *Asteroids II*, ed. R. Binzel, T. Gehrels, & M. Matthews (Tucson: Univ. Arizona Press), 524  
 Brown, M., Schaller, E., Roe, H., Rabinowitz, D., & Trujillo, C. 2006, *ApJ*, 643, L61  
 Brown, M., Trujillo, C., & Rabinowitz, D. 2005, *ApJ*, 635, L97  
 Buie, M., Tholen, D., & Wasserman, L. 1997, *Icarus*, 125, 233  
 Buratti, B., et al. 2003, *Icarus*, 162, 171  
 Carraro, G., Maris, M., Bertin, D., & Parisi, M. 2006, *A&A*, 460, L39  
 Chandrasekhar, S. 1969, *Ellipsoidal Figures of Equilibrium* (New Haven: Yale Univ. Press)  
 Cruikshank, D., Barucci, M., Emery, J., Fernandez, Y., Grundy, W., Noll, K., & Stansberry, J. 2006, in *Protostars and Planets V*, ed. B. Reipurth, D. Jewitt, & K. Keil (Tucson: Univ. Arizona Press), in press  
 Cruikshank, D., Stansberry, J., Emery, J., Fernandez, Y., Werner, M., Trilling, D., & Rieke, G. 2005, *ApJ*, 624, L53  
 Davis, D., & Farinella, P. 1997, *Icarus*, 125, 50  
 de Bergh, C., Delsanti, A., Tozzi, G., Dotto, E., Doressoundiram, A., & Barucci, M. 2005, *A&A*, 437, 1115  
 Doressoundiram, A., Peixinho, N., Doucet, C., Mousis, O., Barucci, M., Petit, J., & Veillet, C. 2005, *Icarus*, 174, 90  
 Elliot, J., et al. 2003, *Nature*, 424, 165  
 Farinella, P., Davis, D., Paolicchi, P., Cellino, A., & Zappala, V. 1992, *A&A*, 253, 604  
 Farinella, P., & Paolicchi, P. 1982, *Icarus*, 52, 409  
 Hicks, M., Simonelli, D., & Buratti, B. 2005, *Icarus*, 176, 492  
 Holsapple, K. 2001, *Icarus*, 154, 432  
 Hubbard, W. 2003, *Nature*, 424, 137  
 Jewitt, D., & Luu, J. 1998, *AJ*, 115, 1667  
 ———. 2004, *Nature*, 432, 731  
 Jewitt, D., & Sheppard, S. 2002, *AJ*, 123, 2110  
 Lacerda, P., & Luu, J. 2006, *AJ*, 131, 2314  
 Landolt, A. 1992, *AJ*, 104, 340  
 Leone, G., Farinella, P., Paolicchi, P., & Zappala, V. 1984, *A&A*, 140, 265  
 Licandro, J., Pinilla-Alonso, N., Pedani, M., Oliva, E., Tozzi, G., & Grundy, W. 2006, *A&A*, 445, L35  
 Muinonen, K., Piironen, J., Shkuratov, Y., Ovcharenko, A., & Clark, B. 2002, in *Asteroids III*, ed. W. Bottke et al. (Tucson: Univ. Arizona Press), 123  
 Ortiz, J., Gutierrez, P., Santos-Sanz, P., Casanova, V., & Sota, A. 2006, *A&A*, 447, 1131  
 Rabinowitz, D., Schaefer, B., & Tourtellotte, S. 2007, *AJ*, 133, 26  
 Rabinowitz, D., et al. 2006, *ApJ*, 639, 1238  
 Romanishin, W., & Tegler, S. 2005, *Icarus*, 179, 523  
 Sheppard, S., & Jewitt, D. 2002, *AJ*, 124, 1757  
 ———. 2003, *Earth Moon Planets*, 92, 207  
 ———. 2004, *AJ*, 127, 3023  
 Sicardy, B., et al. 2003, *Nature*, 424, 168  
 Spencer, J., Stansberry, J., Trafton, L., Young, E., Binzel, R., & Croft, S. 1997, in *Pluto and Charon*, ed. S. Stern & D. Tholen (Tucson: Univ. Arizona Press), 435  
 Stansberry, J., Grundy, W., Margot, J., Cruikshank, D., Emery, J., Rieke, G., & Trilling, D. 2006, *ApJ*, 643, 556  
 Stellingwerf, R. 1978, *ApJ*, 224, 953  
 Trilling, D., & Bernstein, G. 2006, *AJ*, 131, 1149  
 Trujillo, C., Brown, M., Barkume, K., Schaller, E., & Rabinowitz, D. 2007, *ApJ*, 655, 1172  
 Trujillo, C., Jewitt, D., & Luu, J. 2001, *AJ*, 122, 457  
 Weidenschilling, S. 1981, *Icarus*, 46, 124